Am J Cancer Res 2020;10(1):114-130
www.ajcr.us /ISSN:2156-6976/ajcr0104106

Original Article

TRIM21 overexpression promotes tumor progression by regulating cell proliferation, cell migration and cell senescence in human glioma

Zhipeng Zhao[1,8*], Yuqi Wang[1*], Dapeng Yun[2], Qilin Huang[3], Delong Meng[4], Qing Li[5], Pingzhao Zhang[6], Chenji Wang[7], Hongyan Chen[1], Daru Lu[1,9]

[1]State Key Laboratory of Genetic Engineering and MOE Engineering Research Center of Gene Technology, School of Life Sciences, Fudan University, Shanghai 200438, China; [2]Department of Pharmacology, The University of Texas Southwestern Medical Center, Dallas TX75390, USA; [3]Department of Neurosurgery, Shanghai Institute of Neurosurgery, Changzheng Hospital, Second Military Medical University, Shanghai 200003, China; [4]Department of Molecular Biology, The University of Texas Southwestern Medical Center, Dallas TX75390, USA; [5]Shanghai Center for Clinical Laboratory, 528 Hongshan Road, Pudong District, Shanghai 200126, China; [6]Fudan University Shanghai Cancer Center and Institutes of Biomedical Sciences, Shanghai Medical College, Shanghai 200032, China; [7]State Key Laboratory of Genetic Engineering, Collaborative Innovation Center for Genetics and Development, School of Life Sciences, Fudan University, Shanghai 200438, China; [8]School of Physical Education, Xizang Minzu University, Xianyang 712000, Shaanxi, China; [9]Key Laboratory of Birth Defects and Reproductive Health of National Health and Family Planning Commission, Chongqing Population and Family Planning, Science and Technology Research Institute, Chongqing 400020, China. [*]Equal contributors.

Received October 28, 2019; Accepted December 6, 2019; Epub January 1, 2020; Published January 15, 2020

Abstract: Molecular biomarkers combined with histopathological examination are of critical importance in the diagnosis and treatment of gliomas. Although recent studies have shown that many tripartite motif-containing (TRIM) family proteins could regulate the cell cycle, cell proliferation, and differentiation in cancers, the precise role of TRIM21 has been unknown in glioma. In this study, we analyzed TRIM21, which was upregulated in gliomas and identified its role in tumor proliferation, migration and drug resistance. By using immunohistochemical analysis, we found that the expression level of TRIM21 was upregulated in glioma specimens and the higher expression level of TRIM21 was associated with poorer clinical outcomes in glioma patients. Moreover, we demonstrated that TRIM21 could act as a regulator of the proliferation, cell cycle, and migration of glioma cells by gain- and loss-of function assays in vitro. In vivo, TRIM21 could also modulate glioma progression in murine intracranial xenografts. Furthermore, we found that TRIM21 suppressed cellular senescence via the p53-p21 pathway, and increased drug resistance in glioma cells by RNA-seq analysis, SA-β-Gal activity assay, and Cell Counting Kit-8 (CCK-8) assay. These results indicated that TRIM21 is a novel regulator in the diagnosis, prognosis, and therapy of gliomas.

Keywords: Glioma, TRIM21, prognosis, cell senescence, p53-p21 pathway, drug resistance

Introduction

Glioma is the most common primary malignant tumor in the brain and other areas of the central nervous system (CNS) in adults. Glioblastoma (GBM), which is a high-grade subtype, account for 56.6% of gliomas [1]. The median survival of patients initially diagnosed with GBM is less than 15 months [2, 3], even with ideal treatment with maximal surgical resection and subsequent chemoradiotherapy. Molecular and histological parameters are now being combined for the diagnosis and treatment plan of patients with glioma in the revised 2016 WHO classification of CNS tumors [4]. Thus, effective novel biomarkers for the accurate identification and the appropriate therapy designs of gliomas remain crucial anti-tumor requirements.

The tripartite motif-containing (TRIM) family members contain a structurally conserved N-terminal with Really Interesting New Gene (RING) motif followed by one or two zinc-finger

domains called B-boxes and a coiled-coil (CC) domain [5-7]. As a member of this family, TRIM21 also contains PRY and SPRY domains at the C-terminus. Like any other family members, TRIM21 is an E3 ligase via its RING domain [8]. It is an autoantigen related to autoimmune diseases, such as systemic lupus erythematosus and Sjögren's syndrome [9, 10].

TRIM21 regulates innate immune signaling through its E3 ligase function. It negatively regulates the innate immune response to intracellular double-stranded DNA and DNA viruses by ubiquitination and degradation of DDX41 [11]. Furthermore, IRF3, IRF5, and other interferon response factors are ubiquitination substrates of TRIM21. They are regulated by a TRIM21-mediated proteasome degradation pathway [12-14]. TRIM21 could also regulate cellular processes. It reduces B-cell proliferation and facilitates apoptotic cell death [15]. Moreover, it induces cell apoptosis through suppressing anti-apoptotic protein Bcl-2 and GSK3β expression as a proapoptotic molecule [16, 17].

Previous studies suggest that TRIM21 may play a role in tumor development. Recent studies have explored the relationships between TRIM21 expression and tumor prognosis. High- and low-level expressions of TRIM21 are associated with good and poor prognosis, respectively, in breast cancer [18, 19]. In two studies about hepatocellular carcinoma and diffuse large B-cell lymphoma, the reduced expression of TRIM21 implicated a poor prognosis [20, 21]. TRIM21 can increase the resistance of colon cancer cells to cisplatin by down-regulating Par-4 levels and ubiquitylating FASN to regulate its protein [22, 23]. Interestingly, TRIM21 could destabilize p53, a vital tumor-suppressor protein, by mediating the ubiquitination and degradation of GMPS or HuR [24, 25]. However, the expression and functions of TRIM21 in gliomas have not been reported yet.

This study investigated the expression, functions, and prognostic value of TRIM21 in gliomas. We found that TRIM21 expression was frequently higher in glioma tissues than in normal brain tissues. TRIM21 could regulate cell proliferation and migration of gliomas. It regulated cell senescence through the p53-p21 pathway in glioma cells. Our research suggests that TRIM21 is a novel diagnostic, prognostic, and therapeutic factor in gliomas.

Results

TRIM21 is elevated in human gliomas

To investigate the expression of TRIM21 in gliomas, the expression levels of TRIM21 protein were examined by immunohistochemical staining performed on the Chinese tissue microarray (TMA), containing 264 gliomas and 16 controls. As shown in **Figure 1A**, **1B** and Table S1, the immunoreactivity of TRIM21 was significantly elevated in LGG (low grade glioma) and HGG (high grade glioma) samples, and increased according to WHO grade. Furthermore, similar results could be seen between normal brain tissues and gliomas of different WHO grade or histological grouping (**Figure 1B**). We further determined whether the *TRIM21* gene was also increased at the transcriptional level. We examined its mRNA level in a cohort of 17 normal brain tissues and 41 glioma specimens. Consistently, the mRNA expression of *TRIM21* was also significantly increased in different WHO grade gliomas (**Figure 1C**). Moreover, the result was further confirmed in TCGA, CGGA and Rembrandt cohorts (**Figure 1D-F**). Taken together, our findings suggested that TRIM21 is elevated in human gliomas.

TRIM21 serves as a prognostic factor

To explore the relationship between TRIM21 expression and the clinical prognosis of patients with glioma, we first examined the prognostic significance of TRIM21 protein expression in a Chinese TMA cohort. Kaplan-Meier analysis was performed, and the results showed that in all patients with glioma, those with high TRIM21 expression had a markedly shorter overall survival (OS) and progression-free survival (PFS) than those with low TRIM21 expression (**Figure 2A**). As higher tumor grade is an indubitable risk factor for glioma, we further conducted similar analysis in patients with HGG and GBM. As shown in **Figure 2B** and **2C**, high TRIM21 expression could also predict significantly unfavorable OS and PFS in patients with HGG and GBM. Similar analysis performed in the CGGA, TCGA, and Rembrandt cohorts revealed that, higher *TRIM21* mRNA expression could significantly predict worse OS and PFS for all gliomas (**Figures 2E** and S1), HGGs (**Figure 2F**) and GBMs (**Figure 2D**).

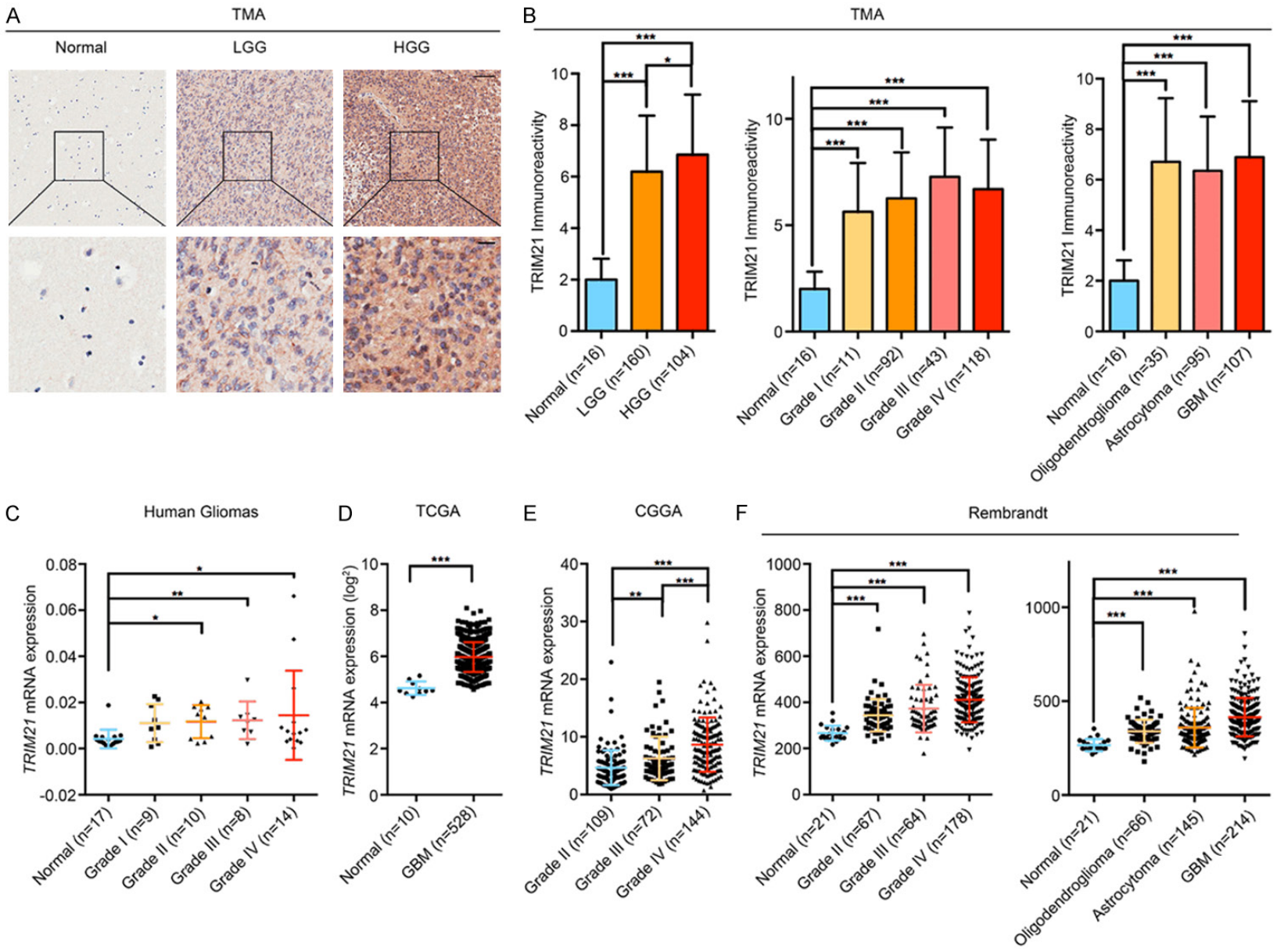
A
TMA
Normal
LGG
HGG
B
TMA
TRIM21 Immunoreactivity
Normal (n=16)
LGG (n=160)
HGG (n=104)
Grade I (n=11)
Grade II (n=92)
Grade III (n=43)
Grade IV (n=118)
Oligodendroglioma (n=35)
Astrocytoma (n=95)
GBM (n=107)
C
Human Gliomas
TRIM21 mRNA expression
Normal (n=17)
Grade I (n=9)
Grade II (n=10)
Grade III (n=8)
Grade IV (n=14)
D
TCGA
TRIM21 mRNA expression (log2)
Normal (n=10)
GBM (n=528)
E
CGGA
TRIM21 mRNA expression
Grade II (n=109)
Grade III (n=72)
Grade IV (n=144)
F
Rembrandt
TRIM21 mRNA expression
Normal (n=21)
Grade II (n=67)
Grade III (n=64)
Grade IV (n=178)
Oligodendroglioma (n=66)
Astrocytoma (n=145)
GBM (n=214)

Figure 1. Protein expression and mRNA transcript of *TRIM21* gene are elevated in human gliomas. (A) TRIM21 protein expression was analyzed by immunohistochemistry staining and representative staining images in normal brains and gliomas. LGG, Low Grade Gliomas; HGG, High Grade Gliomas. Scale bar, 20 μm and 10 μm respectively. (B) Immunoreactivity scores of TRIM21 staining in normal brains samples and different gliomas. Data are shown as means ± SEM. *, $P<0.05$; ***, $P<0.001$. (C) *TRIM21* mRNA expression was analyzed by real time RT-PCR assays in human gliomas of different WHO grades and normal brains, and *GAPDH* was used as an internal control. Data are shown as means ± SEM. *, $P<0.05$; **, $P<0.01$. (D-F) *TRIM21* gene expression was compared between gliomas and normal brains in TCGA (D), CGGA (E) and Rembrandt (F) cohorts. Data are shown as means ± SEM. **, $P<0.01$; ***, $P<0.001$.

Univariate and multivariate Cox regression analyses were also performed to examine the independence of the prognostic value of TRIM21 protein expression. As shown in **Table 1**, after correction for clinical characteristics suggested to be significant prognostic factors in univariate Cox regression, high TRIM21 protein expression was an independent risk predictor of both OS and PFS for all gliomas, HGGs, and GBMs in the Chinese TMA cohort. Together, our findings indicate that TRIM21 serves as a prognostic factor in all gliomas, HGGs and GBMs.

TRIM21 promotes cell growth and migration in vitro

To further explore the biological significance of TRIM21 in glioma, TRIM21-overexpressed or depleted U87-MG and U251 cells were established by lentivirus infection with optimized lentivirus vectors (**Figures 3A**, S2A and S2B). As determined by CCK-8 assays, TRIM21-overexpressed U87-MG and U251 cells displayed a faster growth rate than the controls; targeting TRIM21 by shRNAs markedly inhibited cell proliferation, and similar results were obtained in U373 cells (**Figures 3B** and S2C). Consistent results in U251 cells were observed in colony formation assays (Figure S2D). We further examined whether the cell cycle was regulated by TRIM21 in glioma. Cell cycle analyses and EdU assays demonstrated that the percentage of G1 phase cells was significantly reduced with TRIM21 overexpression and elevated with TRIM21 depletion, on the contrary, the percentage of S phase cells was significantly elevated with TRIM21 overexpression and reduced with TRIM21 depletion (**Figure 3C-E**). Moreover, transwell and wound healing assays displayed that TRIM21 overexpression markedly promoted cell migration, whereas TRIM21 depletion depressed cell migration (**Figure 4A-D**). Taken together, our results indicated that TRIM21 regulates glioma cell growth and migration in vitro.

TRIM21 promotes glioma growth in vivo

Our data indicated that TRIM21 controls glioma cells survival in vitro and suggested that it might play an important role in the modulation of glioma progression. To verify the impact of TRIM21 in glioma, we conducted an in vivo experiment with intracranial xeno-transplanted tumor models. In intracranial xenograft mice, tumor progression was monitored by bioluminescence imaging technique on day 14, 20, and 26 after implantation. Xenografts carrying TRIM21-overexpressed U87-MG cells showed a significant increase in signal compared with the control group. On the contrary, mice bearing TRIM21-depleted U87-MG cells showed a drastic regression of tumor growth compared with the control group (**Figure 5A**). Survival rates of different groups of intracranial xenograft mice were described by the survival curve. As shown in **Figure 5B**, compared with the control group, mice injected with TRIM21-overexpressed U87-MG cells and TRIM21-depleted U87-MG cells exhibited shorter and longer OS time, respectively. For a pathological form of the intracranial tumor, representative paralleled HE-stained images from each group are shown in **Figure 5C**. Immunostaining analyses revealed an elevation of Ki-67 expression in tumors derived from TRIM21-overexpressed U87-MG cells (**Figure 5D** and **5E**).

TRIM21 suppresses cell senescence through the p53-p21 pathway in glioma cells

To further elucidate the mechanism by which TRIM21 modulates glioma progression, RNA isolated from U87-MG cells infected with lentivirus expressing shLuc and shTRIM21 was subjected to transcriptional RNA sequencing profiling. A total of 116 million paired-end reads with average of 19 million reads per sample were generated from RNA sequencing, and a summary of their transcriptome statistics is

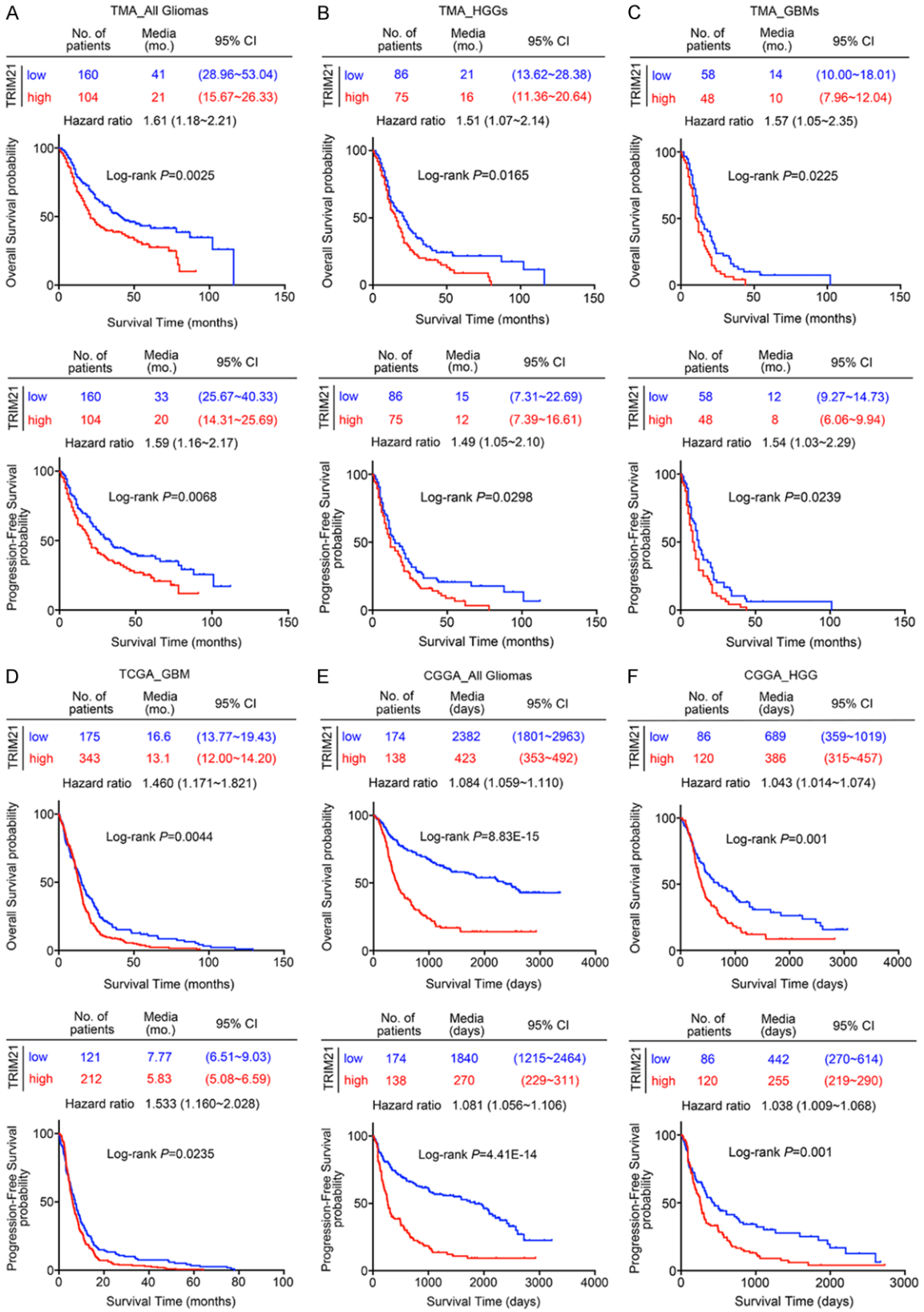

Figure 2. High expression of *TRIM21* predicts a poor clinical outcome in human gliomas. A. Kaplan-Meier survival curves were plotted according to different TRIM21 immunoreactivity level for overall survival (upper panel) and progression-free survival (lower panel) of all glioma patients in the Chinese TMA cohort. B. Kaplan-Meier survival curves

were plotted according to different TRIM21 immunoreactivity level for overall survival (upper panel) and progression-free survival (lower panel) of HGG patients in the Chinese TMA cohort. C. Kaplan-Meier survival curves were plotted according to different TRIM21 immunoreactivity level for overall survival (upper panel) and progression-free survival (lower panel) of GMB patients in the Chinese TMA cohort. D. Kaplan-Meier survival curves were plotted according to different *TRIM21* gene expression for overall survival (upper panel) and progression-free survival (lower panel) of GBM patients in the TCGA cohort. E. Kaplan-Meier survival curves were plotted according to different *TRIM21* gene expression for overall survival (upper panel) and progression-free survival (lower panel) of all glioma patients in the CGGA cohort. F. Kaplan-Meier survival curves were plotted according to different *TRIM21* gene expression for overall survival (upper panel) and progression-free survival (lower panel) of HGG patients in the CGGA cohort.

Table 1. Univariate and multivariate Cox regression of TRIM21 immunoreactivity for overall survival and progression-free survival in all glioma patients, HGG patients and GBM patients in the Chinese TMA cohort

Patients groups and clinical characteristics	Univariate Cox Regression		Multivariate Cox Regression	
	HR (95% CI)	*P*	HR (95% CI)	*P*
All glioma patients (n=246)				
OS				
Age (≥45 vs. <45)	2.43 (1.69-3.49)	2E-06	1.75 (1.19-2.56)	0.004
Necrosis (Yes vs. No)	1.87 (1.26-2.78)	0.002		0.407
Grade (high vs. low)	5.66 (3.78-8.48)	4.26E-17	2.67 (1.57-4.54)	3.07E-04
Lineage (GBM vs. other)	6.21 (4.46-8.64)	3.60E-27	3.73 (2.46-5.66)	6.78E-10
TRIM21 expression (high vs. low)	1.61 (1.18-2.21)	0.003	1.53 (1.11-2.11)	0.01
PFS				
Age (≥45 vs. <45)	2.57 (1.79-3.70)	3.65E-07	1.87 (1.28-2.75)	0.001
Necrosis (Yes vs. No)	2.04 (1.38-3.04)	3.98E-04		0.091
Grade (high vs. low)	5.89 (3.93-8.83)	8.52E-18	2.89 (1.70-4.89)	8.2E-05
Lineage (GBM vs. other)	6.17 (4.43-8.59)	5.40E-27	3.46 (2.29-5.22)	3.52E-09
TRIM21 expression (high vs. low)	1.59 (1.16-2.17)	0.004	1.45 (1.05-2.00)	0.023
High Grade Glioma (n=161)				
OS				
Age (≥45 vs. <45)	1.87 (1.27-2.76)	0.002	1.57 (1.04-2.38)	0.032
Resection (>98% vs. <98%)	1.40 (1.05-1.86)	0.021		0.052
Radiotherapy (Yes vs. No)	0.64 (0.44-0.91)	0.013		0.061
Lineage (GBM vs. other)	3.32 (2.22-4.95)	4.23E-09	3.69 (2.41-5.65)	2.11E-09
TRIM21 expression (high vs. low)	1.51 (1.07-2.135)	0.019	1.82 (1.28-2.60)	0.001
PFS				
Age (≥45 vs. <45)	2.03 (1.38-3.00)	3.69E-04	1.70 (1.12-2.58)	0.013
Gender (male vs. female)	0.67 (0.47-0.95)	0.027	0.64 (0.43-0.96)	0.03
Radiotherapy (Yes vs. No)	3.20 (2.15-4.75)	9.40E-09	3.53 (2.31-5.39)	5.52E-09
Lineage (GBM vs. other)	0.68 (0.48-0.96)	0.029	0.58 (0.40-0.85)	0.005
TRIM21 expression (high vs. low)	1.49 (1.05-2.10)	0.024	1.79 (1.25-2.56)	0.001
GBM (n=106)				
OS				
Radiotherapy (Yes vs. No)	0.63 (0.41-0.95)	0.029		0.058
TRIM21 expression (high vs. low)	1.57 (1.05-2.35)	0.028	1.67 (1.11-2.51)	0.014
PFS				
Age (≥45 vs. <45)	1.60 (1.03-2.49)	0.037	1.59 (1.01-2.51)	0.048
Radiotherapy (Yes vs. No)	0.65 (0.43-0.99)	0.046		0.166
TRIM21 expression (high vs. low)	1.54 (1.03-2.29)	0.036	1.60 (1.06-2.40)	0.025

Abbreviations: OS, overall survival; PFS, progression-free survival; HR: hazard ratio; CI, confidence interval.

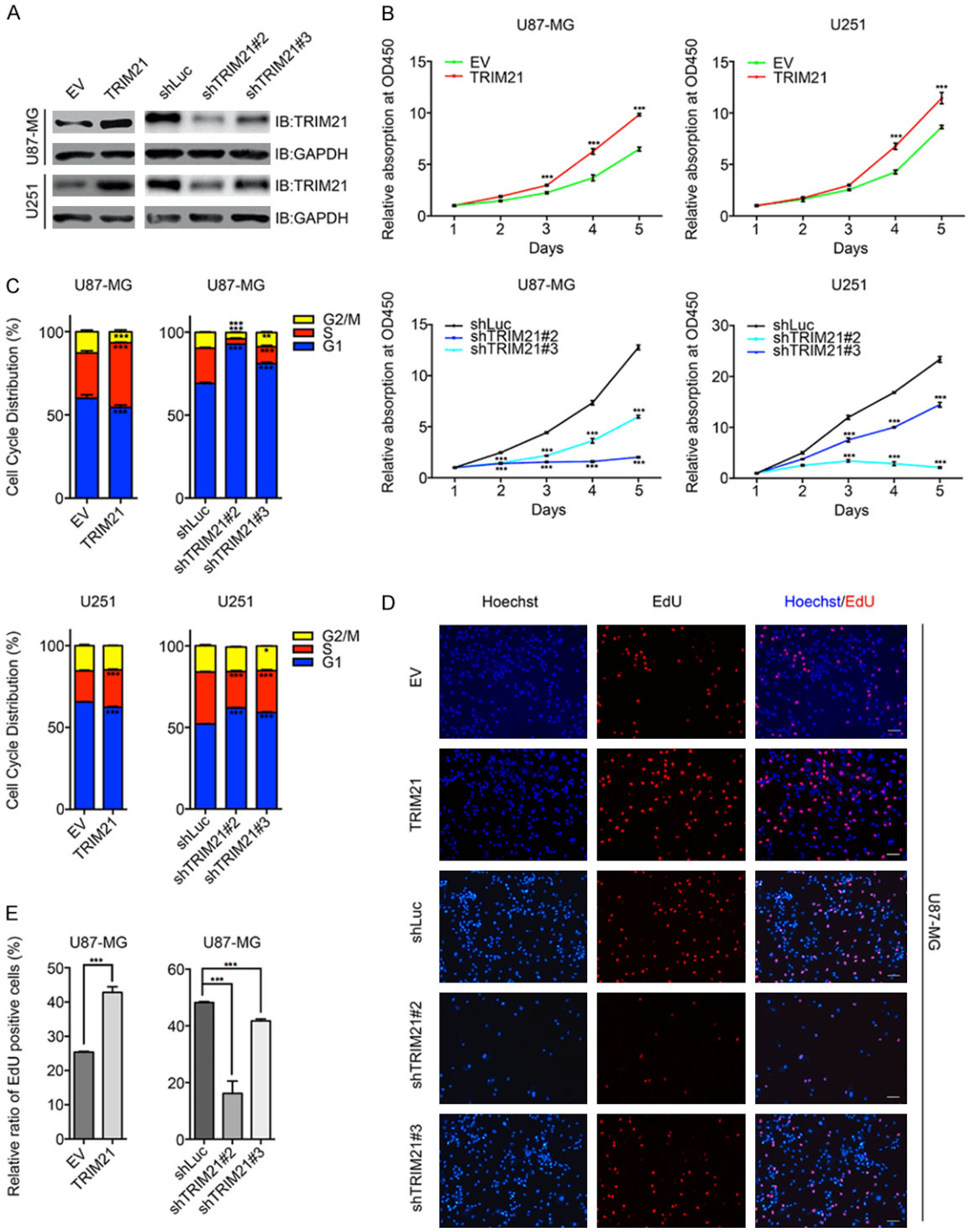

Figure 3. TRIM21 promotes cell growth in glioma cells. A. Western blot of indicated proteins in WCLs of U87-MG and U251 cells infected with lentivirus expressing indicated plasmids or shRNAs for 48 hr. B. CCK-8 cell proliferation analyses of U87-MG and U251 cells infected with lentivirus expressing indicated plasmids or shRNAs. Data are shown as means ± SD (n=3). ***, $P<0.001$. C. Cell cycle analyses of U87-MG and U251 cells infected with lentivirus expressing indicated plasmids or shRNAs. Data are shown as means ± SD (n=3). *, $P<0.05$, **, $P<0.01$, ***, $P<0.001$. D. EdU incorporation analyses of U87-MG cells infected with lentivirus expressing indicated plasmids or shRNAs. Scale bar, 20 μm. E. The quantitative analyses of EdU incorporation assays. Data are shown as means ± SD (n=3). ***, $P<0.001$.

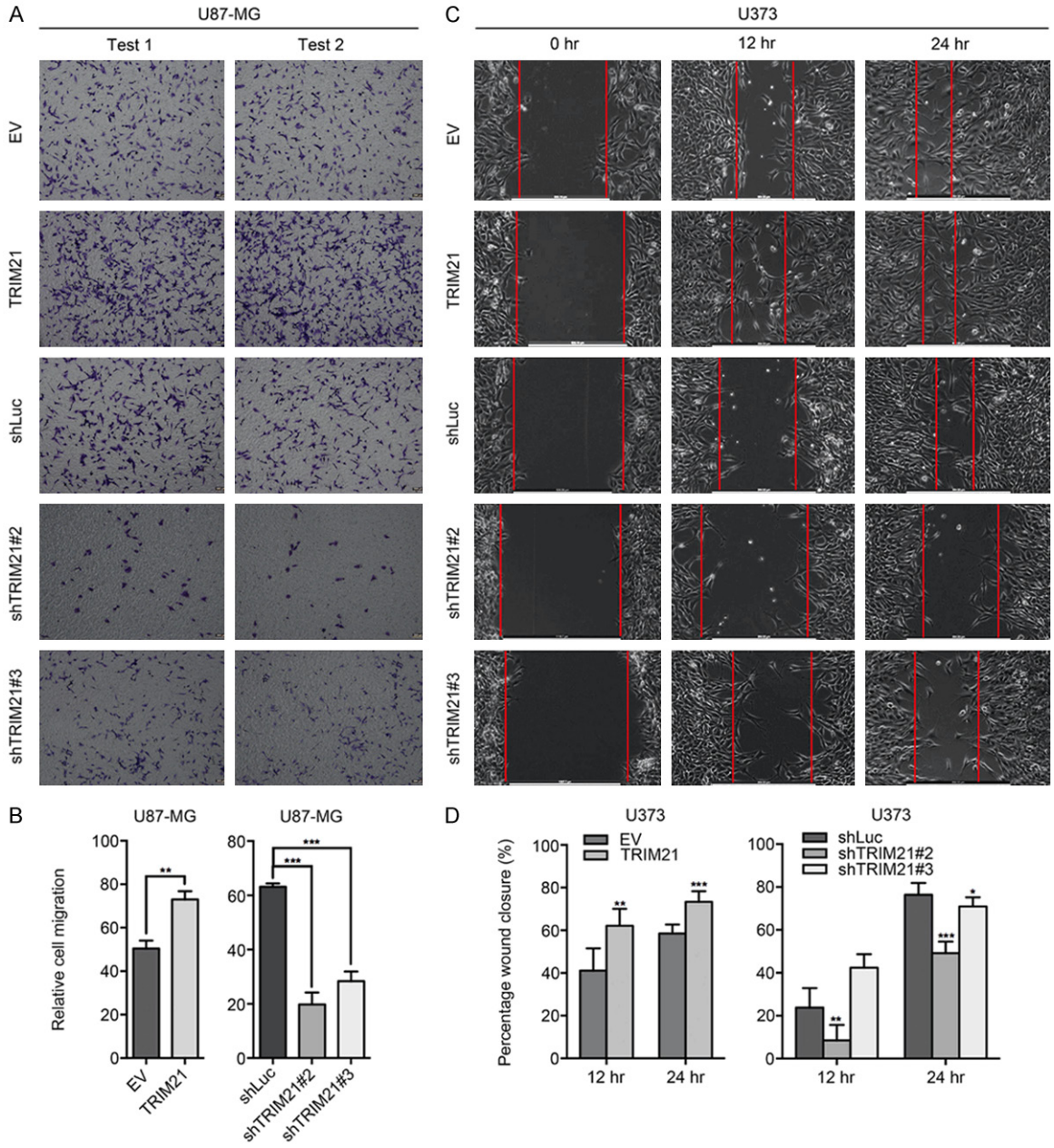

Figure 4. TRIM21 promotes cell migration in vitro. A. Transwell migration analyses of U87-MG cells infected with lentivirus expressing indicated plasmids or shRNAs. Two representative images were shown. B. The quantitative analyses of transwell migration assays. Data are shown as means ± SD (n=3). **, $P<0.01$, ***, $P<0.001$. C. Wound healing analyses of U373 cells infected with lentivirus expressing indicated plasmids or shRNAs. D. The quantitative analyses of wound healing assays. Data are shown as means ± SD (n=3). *, $P<0.05$, **, $P<0.01$, ***, $P<0.001$.

shown in Table S2. Meanwhile, comparing shLuc with shTRIM21 U87-MG cells, a total of 1 601 differentially expressed genes (DEGs) were identified on the basis of p-value ≤0.05. Among all DEGs, 773 and 828 genes were downregulated and upregulated, respectively. Gene Ontology analysis showed that the identified upregulated genes were mainly involved in endoplasmic reticulum unfolded protein response, response to topologically incorrect protein, cellular response to unfolded protein, and cellular response to topologically incorrect protein biological processes (**Figure 6A**). These biological processes are related to the E3 ligase function of TRIM21. Moreover, a number of identified upregulated genes were involved

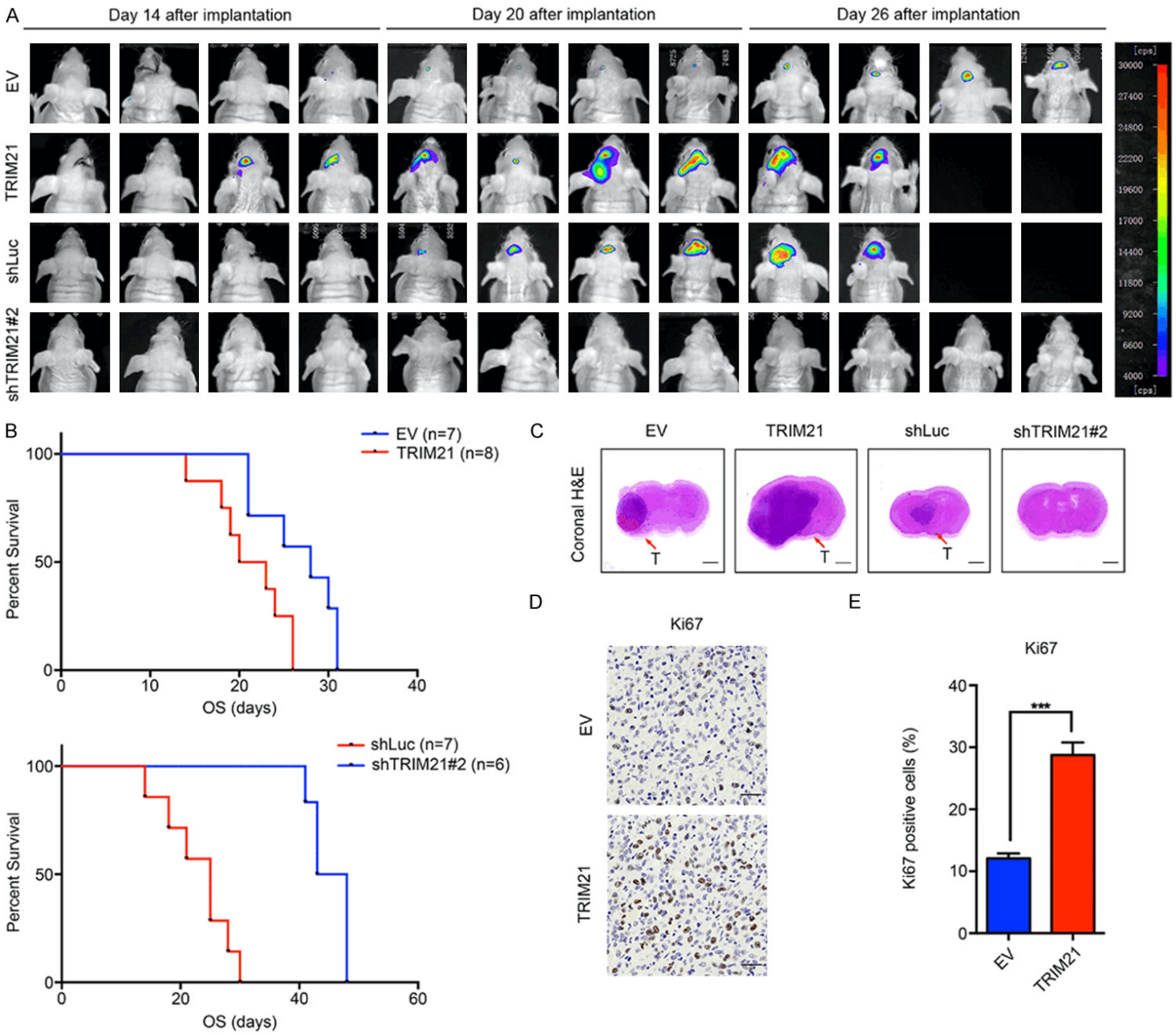
A
Day 14 after implantation
Day 20 after implantation
Day 26 after implantation
EV
TRIM21
shLuc
shTRIM21#2
[cps]
30000
27400
24800
22200
19600
17000
14400
11800
9200
6600
4000
[cps]
B
EV (n=7)
TRIM21 (n=8)
Percent Survival
OS (days)
shLuc (n=7)
shTRIM21#2 (n=6)
Percent Survival
OS (days)
C
EV
TRIM21
shLuc
shTRIM21#2
Coronal H&E
T
D
Ki67
EV
TRIM21
E
Ki67
Ki67 positive cells (%)
***
EV
TRIM21

Figure 5. TRIM21 promotes glioma growth in intracranial xenografts. A. Representative pseudocolor bioluminescence images of intracranial mice of U87-MG cells with lentivirus expressing indicated plasmids or shRNAs on the days as indicated. B. Kaplan-Meier curves determine the survival rate of mice with intracranial xenografts derived from U87-MG cells with lentivirus expressing indicated plasmids or shRNAs. C. Representative H&E staining for a pathological form of the intracranial tumor from each group; T, tumor. Scale bar, 20 μm. D, E. IHC analyses of Ki67 expression in intracranial tumors developed from U87-MG cells with lentivirus expressing indicated plasmids. Data are shown as means ± SD (n=3). ***, $P<0.001$. Scale bar, 20 μm.

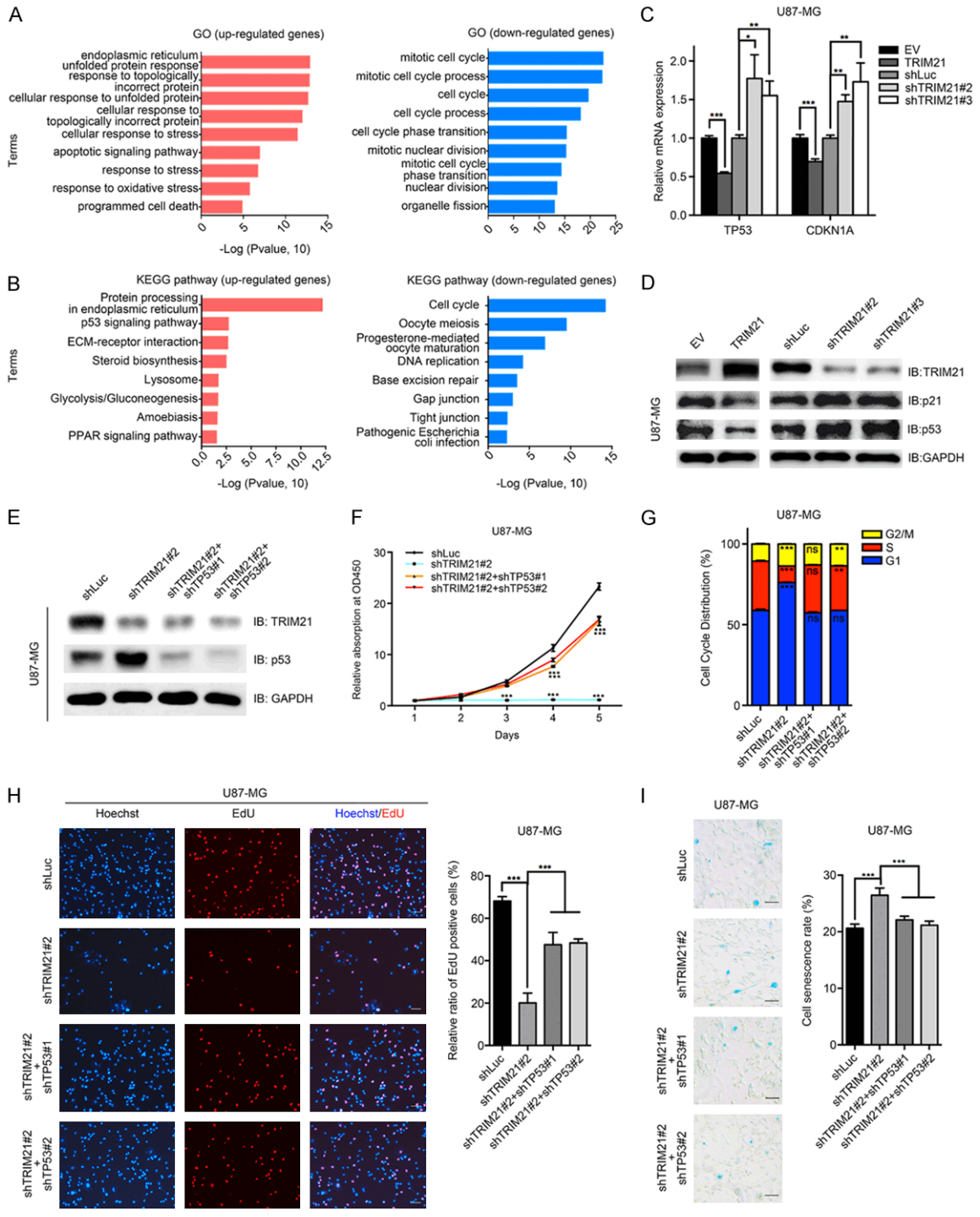

Figure 6. TRIM21 suppresses cell senescence through p53-p21 pathway in glioma cells. (A, B) Gene Otology (A) and KEGG pathway (B) enrichment analyses of identified DEGs (Differentially Expressed Genes) by RNA-seq from U87-MG cells infected with lentivirus expressing shLuc and shTRIM21#2 for 48 hr. (C) qRT-PCR assessments of *TP53* and *CDKN1A* mRNA expression in U87-MG cells infected with lentivirus expressing indicated plasmids or shRNAs. Data are shown as means ± SD (n=3). *, $P<0.05$, **, $P<0.01$, ***, $P<0.001$. (D, E) Western blot of indicated proteins in WCLs of U87-MG cells infected with lentivirus expressing indicated plasmids or shRNAs for 48 hr. (F) CCK-8 cell proliferation analyses of U87-MG cells infected with lentivirus expressing indicated shRNAs. Data are shown as means ± SD (n=3). ***, $P<0.001$. (G) Cell cycle analyses of U87-MG cells infected with lentivirus expressing indicated shRNAs. Data are shown as means ± SD (n=3). ns, not significant, **, $P<0.01$, ***, $P<0.001$. (H) EdU incorporation analyses of U87-MG cells infected with lentivirus expressing indicated shRNAs. Scale bar, 20 μm. Data are shown as means ± SD (n=3). ***, $P<0.001$. (I) SA-β-Gal activity assays of U87-MG cells infected with lentivirus expressing indicated shRNAs for 48 hr. Scale bar, 20 μm. Data are shown as means ± SD (n=3). ***, $P<0.001$.

in cellular response to stress, apoptotic signaling pathway, response to stress and response to oxidative stress biological processes (**Figure 6A**). In addition, downregulated genes were mainly involved in mitotic cell cycle, cell cycle process, cell cycle phase transition, and DNA repair (**Figure 6A**). These biological processes are closely related to cell senescence. More importantly, KEGG analysis revealed that the identified DEGs were significantly enriched in protein processing in endoplasmic reticulum pathway, p53 signaling pathway, and cell cycle pathway (**Figure 6B**).

Because p53-p21 is one of the major pathways that mediate aging, we quantified the mRNA and protein levels of *TP53* and *CDKN1A* in the pathway. As shown in **Figure 6C** and **6D**, both mRNA and protein levels of *TP53* and *CDKN1A* were significantly reduced in TRIM21-overexpressed U87-MG cells, whereas they were remarkably increased in TRIM21-depleted U87-MG cells. Furthermore, as determined by CCK-8, cell cycle, EdU, and SA-β-Gal staining assays, TRIM21 knockdown promoted cell senescence in U87-MG cells (**Figure 6E-I**). On the contrary, TRIM21-overexpressed U87-MG cells displayed a lower cell senescence rate (Figure S3). Importantly, p53 knockdown could rescue the cell senescence effect of TRIM21 knockdown on glioma cells (**Figure 6E-I**). Taken together, our findings suggested that TRIM21 may modulate glioma progression at least in part, through cell senescence via the p53-p21 pathway.

TRIM21 increases glioma cell resistance to temozolomide (TMZ)

TMZ is a first-line chemotherapeutic drug for GBM. It exerts its effect by causing DNA damage and inhibiting cell division. Several studies have indicated that TMZ resistance is associated with p53 malfunction [26-29]. We performed analyses of *TRIM21* expression stratified by the status of common genetic aberrations of GBM in TCGA cohort. As shown in **Figure 7A** and **7B**, the mRNA expression of *TRIM21* was significantly increased in GBM patients with IDH1 wild type or non-G-CIMP compared with those with IDH1 mutations or G-CIMP. Meanwhile, a similar trend could be seen between MGMT-unmethylated, and MGMT-methylated (**Figure 7C**). Studies have shown that GBM patients with IDH1 mutation, MGMT-methylated and G-CIMP have higher total survival and responsiveness to TMZ treatment [30, 31]. We next examined whether TRIM21 played a critical role in resistance to TMZ therapy. As determined by CCK-8 assays, the overexpression of TRIM21 decreased the sensitivity of U87-MG cells to TMZ, but the depletion of TRIM21 sensitized U87-MG to TMZ (**Figure 7D** and **7E**). Together, our findings indicated that TRIM21 increases the resistance of glioma cells to TMZ, which may be the underlying mechanism in the poor prognosis of glioma patients with high expression of TRIM21.

Discussion

A strong relationship between the expression of TRIM21 and tumor prognosis has been reported in literature [18-21]. Several reports have shown that TRIM21 could also regulate cellular processes [15-17]. Here, we described the high expression of TRIM21 in glioma tissues through microarray analysis. We found that patients with high TRIM21 expression often had a significantly poor OS and PFS. Our study also found that the expression of TRIM21 in glioma tissues was significantly higher than that in normal brain tissues, and exhibited a significant positive correlation with the histopathological grade. However, no relationship was found between TRIM21 expression and

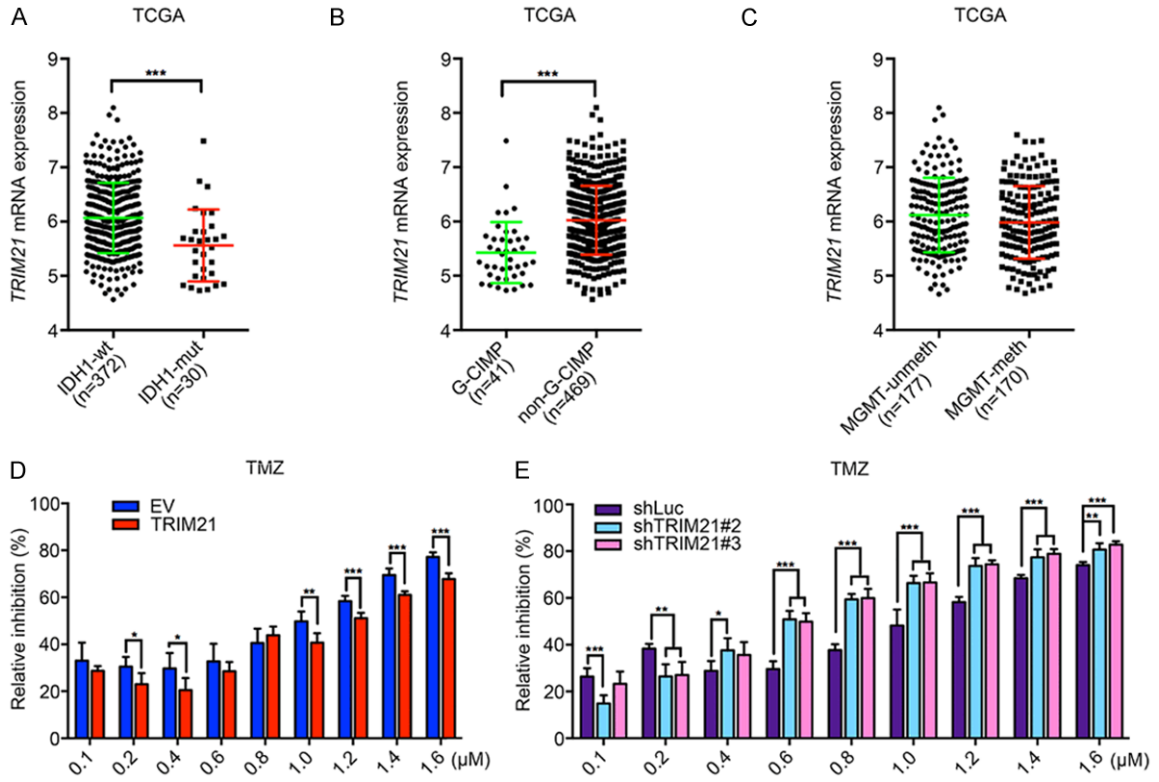

Figure 7. Impact of TRIM21 on cell survival under DNA damage stress induced by TMZ treatment. (A) *TRIM21* gene expression was compared between GBM patients carrying *IDH1*-wt and *IDH1*-mutations in TCGA cohort. (B) *TRIM21* gene expression was compared between GBM patients carrying G-CIMP and non-G-CIMP in TCGA cohort. (C) *TRIM21* gene expression was compared between GBM patients carrying MGMT-unmethylated and MGMT-methylated in TCGA cohort. (D, E) Relative inhibition analyses of U87-MG infected with lentivirus expressing indicated plasmids (D) or shRNAs (E) and treat with TMZ at levels of 0.1, 0.2, 0.4, 0.6, 0.8, 1.0, 1.2, 1.4, 1.6 μM. Data are shown as means ± SD (n=3). *, P<0.05, **, P<0.01, ***, P<0.001. TMZ, temozolomide. G-CIMP, glioma-CpG island methylator phenotype.

gender and age, tumor origin, clinical symptoms, and chemoradiotherapy of patients. All these results confirm that the TRIM21 expression level in glioma tissues could be used as a diagnostic marker and prognostic indicator for patients with glioma.

In this study, we investigated the functions of TRIM21 in glioma both *in vitro* and *in vivo*. We found that TRIM21 overexpression promoted the glioma cell cycle and proliferation, whereas TRIM21 knockdown inhibited cell proliferation and could lead to significant gathering of glioma cells at the G1 phase. Our results suggest that TRIM21 plays an important role in regulating cell cycle and cell proliferation in glioma. We also found that TRIM21 overexpression obviously promoted glioma cell migration, whereas TRIM21 knockdown could inhibit glioma cell migration. Glioma invading the surrounding normal brain tissues is one of the reasons for the poor prognosis. *In vivo* experiments also validated the results mentioned above. We found that TRIM21 overexpression significantly increased tumorigenicity and tumor progression of glioma cells in the intracranial xenograft model in nude mice, whereas TRIM21 knockdown obviously inhibited tumorigenicity and tumor progression. The standard therapeutic method for primary glioma patients is radiation therapy with TMZ, which is the most commonly used anti-glioma chemotherapy, followed by surgery [3]. Another important finding was that TRIM21 knockdown would be as potent at inhibiting GBM cell proliferation as TMZ. In summary, these findings suggest that the functions of TRIM21 in gliomas focus on cell proliferation, cell cycle and invasion, and tumorigenesis and development. Hence, TRIM21 could be a molecular biomarker for glioma treatment.

Previous studies have noted the importance of oncogene-induced senescence as it may be a barrier in tumor development [32-34]. In this study, we found the representative appearance of senescence-associated phenotypes in glioma cells by TRIM21 knockdown. Earlier studies confirmed that TRIM21 could destabilize p53 by ubiquitinating GMPS or HuR [24, 25]. One of the hallmarks of cellular senescence is the induction of anti-proliferative proteins, such as p21 and p53 [35]. We also found that the knockdown of TRIM21 obviously promoted glioma cell senescence by activating the p53-p21 cascade. Although accurate cell prosenescence therapy has a promising potential as part of cancer treatment, it has limitations. Earlier reports have suggested one possibility of the opposing functions of the senescence-associated secretory phenotype, which could enhance HCC growth by NK cell inhibition while senescent hepatocyte-secreted chemokines suppress liver cancer initiation [36]. However, this study confirms that TRIM21 knockdown is associated with cellular senescence, thus, affecting the glioma cell process.

In summary, the present results are significant in at least two major respects. Increased expression of TRIM21 was distinguished in glioma tissues. TRIM21 functions as an oncogene in gliomas by promoting cell proliferation and migration. Furthermore, TRIM21 induces cellular senescence in gliomas through the p53-p21 pathway. Finally, the TRIM21 expression level in glioma is associated with patient prognosis. TRIM21 could be a novel promising target in glioma treatment. Further work is required to establish the viability of TRIM21 as a clinical target in gliomagenesis for early intervention and determine the exact mechanisms responsible for the relevance of TRIM21 upregulation in gliomas.

Materials and methods

Ethics statement

This study complied with the tenets of the Helsinki Declaration and the National Guidelines for Animal Use in Research (China). This study was approved by the Specialty Committee on Ethics of Biomedicine Research of the Second Military Medical University (Shanghai, China, hereafter referred to as 'SMMU'). All animal experiments were conducted with the approval of the Institutional Animal Care and Use Committee of Fudan University. All animal studies were performed according to the Ethics Committee guidelines of Fudan University.

Patient samples

The Chinese tissue microarray (TMA) cohort of human glioma tissue specimens from different WHO grades patients and normal brain tissue samples from trauma patients were obtained from the Department of Neurosurgery in Changzheng Hospital, Second Military Medical University (SMMU) (Shanghai, China), between January 2000 and December 2010. The human gliomas cohort of fresh-frozen tissues from 41 glioma patients and 17 normal controls were collected from the Department of Neurosurgery in Changzheng Hospital, SMMU, between June 2008 and July 2010. Informed consent was provided by each patient. The Specialty Committee on Ethics of Biomedicine Research of SMMU approved the patient sample acquisition.

Antibodies and chemicals

The following antibodies were used: TRIM21 (SC-25351; Santa Cruz), GAPDH (ab9385; Abcam), Ki-67 (9449; Cell Signaling Technology), p53 (9282; Cell Signaling Technology), p21 (ab109520; Abcam). The TRIzol Reagent was purchased from the Invitrogen (Thermo Fisher Scientific, USA). The Cell Counting Kit-8 was purchased from Dojindo Laboratories (Japan). Puromycin was purchased from Sigma. The protease inhibitors cocktail was purchased from the Sigma-Aldrich (USA). The D-luciferin was purchased from Promega (USA). The Lipofectamine 2000 was purchased from Thermo Fisher Scientific (USA).

Cell culture and lentivirus infection

293T and human malignant glioma cell lines (U87-MG, U251, U373) were obtained from the American Type Culture Collection (ATCC). All cells were maintained in DMEM with 10% (v/v) FBS, and were grown at 37°C with 5% CO_2. 293T cells were transiently transfected using Lipofectamine 2000 according to the manufacturer's instructions. pCD513B-1-based gene-overexpression or pll3.7-based gene-knockdown lentiviral vectors and packing constructs

were transfected into 293T cells. Virus-containing supernatant was collected 48 hr. after transfection. U87-MG, U251 and U373 cells were infected with virus-containing supernatant over 48 hr.

Plasmids constructions

TRIM21 cDNA was subcloned into pCD513B-1 lentiviral vector to generate the TRIM21 overexpression plasmid. pll3.7-shRNA plasmids generated by methods described previous [37]. The shRNA sequence of shTRIM21#2: 5'-UGGCAUGGUCUCCUUCUACAA-3'; shTRIM21#3: 5'-CUGCCUUCUUUAUGGGACUUA-3'; shTP53#1: 5'-GUCCAGAUGAAGCUCCCAGAA-3'; shTP53#2: 5'-CGGCGCACAGAGGAAGAGAAU-3'; shLuc: 5'-CAAAUCACAGAAUCGUCGUAU-3'.

Immunohistochemistry assays

The immunohistochemistry assays were performed on TMA and nude mice xenograft tissue to detect TRIM21 and Ki-67 expression by methods described previously. The immunohistochemical staining were scored by two independent pathologists in a blinded manner. The evaluation of the staining density, intensity and the calculation of total immunoreactivity score were described previously. TRIM21 expression was denoted as low (total score ≤6) or high (total score >6) to divide the glioma patients into two groups.

Cell proliferation assays

Cell proliferation rate was determined using Cell Counting Kit-8 (CCK-8) according to the manufacturer's protocol (Dojindo Laboratories, Japan). Briefly, the cells were seeded onto 96-well plates at a density of 1 200 cells per well. During a 4 to 7-d culture periods, 10 μL of the CCK-8 solution was added to cell culture, and incubated for 1 hr. The resulting color was assayed at 450 nm using a microplate absorbance reader (Bio-Rad). Each assay was carried out in triplicate.

Cell cycle analysis

For cell cycle analysis, cells were harvested and washed 48 hr post-treatment with PBS, followed by propidium iodide (50 μg/mL) staining in the presence of RNase (10 μg/mL) for 30 minutes at 4°C in the dark. The fraction of viable cells in G0/G1, S and G2/M phases of cell cycle were determined using a FACs flow cytometer and Cell Quest FACS system (Becton-Dickinson).

EdU assays

EdU assay was performed using the EdU Apollo 567 Cell Tracking Kit (Rib-bio; Guangzhou, China). Treated and control cells (5×10^3/well) were seeded onto 96-well plates and incubated with 5-ethynyl-20-deoxyuridine (EdU; 200 μM) for 2 h at 37°C. Cells were fixed with 4% paraformaldehyde for 20 min, treated with 0.5% TritonX-100 for 10 min, washed with PBS three times, and incubated with 100 μL of Apollo reagent for 30 min. Nuclei were labeled with Hoechst 33342. The percentage of EdU-positive cells was calculated by image J software. Data reported represent the average of three independent experiments.

SA-β-Gal activity assays

SA-β-Gal activity was determined using Sigma SA-β-Gal staining kit according to the manufacturer's protocol. Briefly, the cells were seeded onto 24-well plate 24 or 48 hr before staining. After washing cells with PBS for triple, cells were fixed with the fixation buffer, followed by three washed with PBS and then incubated with SA-β-Gal staining solution at 37°C separated from CO_2 overnight. Cells were visualized and imaged using a microscope (Leica).

Migration assays

Cell migration was determined by Transwell (Costa) migration assay. U87-MG cells were precultured in serum-free medium for 48 hr. 1-3 × 10^4 cells were seeded in serum-free medium in the upper chamber, and the lower chamber was filled with DMEM containing 10% FBS. After 48 hr, the non-migrating cells on the upper chambers were carefully removed with a cotton swab, and the migrated cells underside of the filter stained and counted in nine different fields.

Western blotting

Cell lysates or immunoprecipitates were subjected to SDS-PAGE, and proteins were transferred to nitrocellulose membranes (GE Healthcare Sciences). Membranes were blocked

in Tris-buffered saline (TBS, pH7.4) containing 5% nonfat milk and 0.1% Tween-20, washed twice in TBS containing 0.1% Tween-20 and incubated with primary antibody overnight at 4°C followed by secondary antibody for 1 hr at room temperature. Proteins of interest were visualized using the Enhanced Chemiluminescence (ECL) system (Santa Cruz Biotechnology). Densitometry analysis of protein bands was performed on image J software.

qRT-PCR

Total RNA was isolated from cells or tissues using TRIzol reagent (Thermo Fisher Scientific), and cDNA was reverse-transcribed using the Superscript RT kit (Toyobo), according to the manufacturer's instructions. Quantitative real-time PCR amplification was performed using the THUNDERBIRD SYBR qPCR Mix (Toyobo) on ABI PRISM 7900HT instruments (Applied Biosystems). The amplification was done in a total volume of 10 μL with the following steps: an initial denaturation step at 95°C for 5 min, followed by 40 cycles for denaturation at 95°C for 15 sec and elongation at 60°C for 45 sec. A melting curve analysis of each sample was used to check the specificity of amplification, and each sample was assayed in triplicate. Glyceraldehyde-3-phosphate dehydrogenase (GAPDH) was used as the endogenous control, and the $2^{-\Delta\Delta Ct}$ method was used as relative quantification measure of differential expression. The primer sequences for qRT-PCR used are as follows: TRIM21-F: 5'-CGTTGAGTCCCCTGTAAAGC-3'; TRIM21-R: 5'-CAGGCAGATAGGGCATGTG-3'; TP53-F: 5'-GGAGCCGCAGTCAGATCCTAG-3'; TP53-R: 5'-CAAGGGGGACAGAACGTTG-3'; CDKN1A-F: 5'-TAGCAGCGGAACAAGGAG-3'; CDKN1A-R: 5'-AAACGGGAACCAGGACAC-3'; GAPDH-F: 5'-GAAGGTGAAGGTCGGAGT-3'; GAPDH-R: 5'-GAAGATGGTGATGGGATTTC-3'.

Generation of glioma xenografts in mice

For generation of orthotopic xenografts, 6-week-old female nude mice (SLAC laboratory animal Center, Shanghai, China) were maintained in a barrier facility on high-efficiency particulate air (HEPA)-filtered racks and randomly divided into different experimental groups. U87-MG cells with luciferase expression were infected with TRIM21 overexpression or deletion lentiviruses and their corresponding control lentiviruses. Cells (1×10^6) were surgically implanted into left amygdala of mice brains using a stereotactic apparatus (KDS310, KD Scientific; Holliston, MA, USA). For in vivo BLI, luciferase signals were detected 14, 20, 26 days after transplantation. Mice were intraperitoneally injected with D-luciferin (150 mg/kg) (E1603, Promega) and anesthetized with pentobarbital sodium. After 10 min of substrate administration, images were acquired through the In Vivo Imaging System (IVIS, PerkinElmer, Waltham, MA), and luminescence flux was recorded to assess tumor growth in a blinded fashion. After transplantation, animals were closely followed and euthanized by cervical dislocation when they exhibited central nervous system symptoms, or drastic loss of body weight. Tumors were excised, formalin-fixed, paraffin-embedded, and sectioned for hematoxylin and eosin (HE) staining and IHC. All animal experiments were conducted with the approval of the Institutional Animal Care and Use Committee of Fudan University. All animal studies were performed according to the Ethics Committee guidelines of Fudan University.

Statistics

All data are shown as mean values ± SD/SEM for experiments performed with at least three replicates. The difference between two groups was analyzed using two-tailed Student's t-test unless otherwise specified. Analysis of survival was conducted by Kaplan-Meier survival and Cox regression. * represents $P<0.05$; ** represents $P<0.01$; *** represents $P<0.001$.

Acknowledgements

We also thank Dr. Juxiang Chen (Department of Neurosurgery in Changzheng Hospital, Second Military Medical University), Dr. Hexige Saiyin, Dr. Haoming Chen and Mrs. Taishan Min (School of Life Sciences, Fudan University) for their support.

Disclosure of conflict of interest

None.

Address correspondence to: Daru Lu and Hongyan Chen, State Key Laboratory of Genetic Engineering and MOE Engineering Research Center of Gene Technology, School of Life Sciences, Fudan University, Shanghai 200438, China. Tel: +86-21-

51630619; Fax: +86-21-51630619; E-mail: darulu@163.com (DRL); chenhy@fudan.edu.cn (HYC)

References

[1] Ostrom QT, Gittleman H, Truitt G, Boscia A, Kruchko C and Barnholtz-Sloan JS. Cbtrus statistical report: primary brain and other central nervous system tumors diagnosed in the united states in 2011-2015. Neuro Oncol 2018; 20: iv1-iv86.

[2] Thakkar JP, Dolecek TA, Horbinski C, Ostrom QT, Lightner DD, Barnholtz-Sloan JS and Villano JL. Epidemiologic and molecular prognostic review of glioblastoma. Cancer Epidemiol Biomarkers Prev 2014; 23: 1985-1996.

[3] Stupp R, Mason WP, van den Bent MJ, Weller M, Fisher B, Taphoorn MJ, Belanger K, Brandes AA, Marosi C, Bogdahn U, Curschmann J, Janzer RC, Ludwin SK, Gorlia T, Allgeier A, Lacombe D, Cairncross JG, Eisenhauer E and Mirimanoff RO; European Organisation for Research and Treatment of Cancer Brain Tumor and Radiotherapy Groups; National Cancer Institute of Canada Clinical Trials Group. Radiotherapy plus concomitant and adjuvant temozolomide for glioblastoma. N Engl J Med 2005; 352: 987-996.

[4] Lapointe S, Perry A and Butowski NA. Primary brain tumours in adults. Lancet 2018; 392: 432-446.

[5] Hennig J, Ottosson L, Andresen C, Horvath L, Kuchroo VK, Broo K, Wahren-Herlenius M and Sunnerhagen M. Structural organization and Zn2+-dependent subdomain interactions involving autoantigenic epitopes in the Ring-B-box-coiled-coil (RBCC) region of Ro52. J Biol Chem 2005; 280: 33250-33261.

[6] Reymond A, Meroni G, Fantozzi A, Merla G, Cairo S, Luzi L, Riganelli D, Zanaria E, Messali S, Cainarca S, Guffanti A, Minucci S, Pelicci PG and Ballabio A. The tripartite motif family identifies cell compartments. EMBO J 2001; 20: 2140-2151.

[7] Meroni G and Diez-Roux G. TRIM/RBCC, a novel class of 'single protein RING finger' E3 ubiquitin ligases. Bioessays 2005; 27: 1147-1157.

[8] Wada K and Kamitani T. Autoantigen Ro52 is an E3 ubiquitin ligase. Biochem Biophys Res Commun 2006; 339: 415-421.

[9] Ben-Chetrit E, Chan EK, Sullivan KF and Tan EM. A 52-kD protein is a novel component of the SS-A/Ro antigenic particle. J Exp Med 1988; 167: 1560-1571.

[10] Ben-Chetrit E, Fox RI and Tan EM. Dissociation of immune responses to the SS-A (Ro) 52-kd and 60-kd polypeptides in systemic lupus erythematosus and Sjogren's syndrome. Arthritis Rheum 1990; 33: 349-355.

[11] Zhang Z, Bao M, Lu N, Weng L, Yuan B and Liu YJ. The E3 ubiquitin ligase TRIM21 negatively regulates the innate immune response to intracellular double-stranded DNA. Nat Immunol 2013; 14: 172-178.

[12] Yang K, Shi HX, Liu XY, Shan YF, Wei B, Chen S and Wang C. TRIM21 is essential to sustain IFN regulatory factor 3 activation during antiviral response. J Immunol 2009; 182: 3782-3792.

[13] Higgs R, Ni Gabhann J, Ben Larbi N, Breen EP, Fitzgerald KA and Jefferies CA. The E3 ubiquitin ligase Ro52 negatively regulates IFN-beta production post-pathogen recognition by polyubiquitin-mediated degradation of IRF3. J Immunol 2008; 181: 1780-1786.

[14] Manocha GD, Mishra R, Sharma N, Kumawat KL, Basu A and Singh SK. Regulatory role of TRIM21 in the type-I interferon pathway in Japanese encephalitis virus-infected human microglial cells. J Neuroinflammation 2014; 11: 24.

[15] Espinosa A, Zhou W, Ek M, Hedlund M, Brauner S, Popovic K, Horvath L, Wallerskog T, Oukka M, Nyberg F, Kuchroo VK and Wahren-Herlenius M. The Sjogren's syndrome-associated autoantigen Ro52 is an E3 ligase that regulates proliferation and cell death. J Immunol 2006; 176: 6277-6285.

[16] Jauharoh SN, Saegusa J, Sugimoto T, Ardianto B, Kasagi S, Sugiyama D, Kurimoto C, Tokuno O, Nakamachi Y, Kumagai S and Kawano S. SS-A/Ro52 promotes apoptosis by regulating Bcl-2 production. Biochem Biophys Res Commun 2012; 417: 582-587.

[17] Gao X, Xu F, Zhang HT, Chen M, Huang W, Zhang Q, Zeng Q and Liu L. PKCalpha-GSK3beta-NF-kappaB signaling pathway and the possible involvement of TRIM21 in TRAIL-induced apoptosis. Biochem Cell Biol 2016; 94: 256-264.

[18] Jin Y, Zhang Y, Li B, Zhang J, Dong Z, Hu X and Wan Y. TRIM21 mediates ubiquitination of Snail and modulates epithelial to mesenchymal transition in breast cancer cells. Int J Biol Macromol 2019; 124: 846-853.

[19] Zhou W, Zhang Y, Zhong C, Hu J, Hu H, Zhou D and Cao M. Decreased expression of TRIM21 indicates unfavorable outcome and promotes cell growth in breast cancer. Cancer Manag Res 2018; 10: 3687-3696.

[20] Ding Q, He D, He K, Zhang Q, Tang M, Dai J, Lv H, Wang X, Xiang G and Yu H. Downregulation of TRIM21 contributes to hepatocellular carcinoma carcinogenesis and indicates poor prognosis of cancers. Tumour Biol 2015; 36: 8761-8772.

[21] Brauner S, Zhou W, Backlin C, Green TM, Folkersen L, Ivanchenko M, Löfström B, Xu-

Monette ZY, Young KH, Møller Pedersen L, Boe Møller M, Sundström C, Enblad G, Baecklund E and Wahren-Herlenius M. Reduced expression of TRIM21/Ro52 predicts poor prognosis in diffuse large B-cell lymphoma patients with and without rheumatic disease. J Intern Med 2015; 278: 323-332.

[22] Nguyen JQ and Irby RB. TRIM21 is a novel regulator of Par-4 in colon and pancreatic cancer cells. Cancer Biol Ther 2017; 18: 16-25.

[23] Lin HP, Cheng ZL, He RY, Song L, Tian MX, Zhou LS, Groh BS, Liu WR, Ji MB, Ding C, Shi YH, Guan KL, Ye D and Xiong Y. Destabilization of fatty acid synthase by acetylation inhibits de novo lipogenesis and tumor cell growth. Cancer Res 2016; 76: 6924-6936.

[24] Reddy BA, van der Knaap JA, Bot AG, Mohd-Sarip A, Dekkers DH, Timmermans MA, Martens JW, Demmers JA and Verrijzer CP. Nucleotide biosynthetic enzyme GMP synthase is a TRIM21-controlled relay of p53 stabilization. Mol Cell 2014; 53: 458-470.

[25] Guha A, Ahuja D, Das Mandal S, Parasar B, Deyasi K, Roy D, Sharma V, Willard B, Ghosh A and Ray PS. Integrated regulation of HuR by translation repression and protein degradation determines pulsatile expression of p53 under DNA damage. iScience 2019; 15: 342-359.

[26] Hermisson M, Klumpp A, Wick W, Wischhusen J, Nagel G, Roos W, Kaina B and Weller M. O6-methylguanine DNA methyltransferase and p53 status predict temozolomide sensitivity in human malignant glioma cells. J Neurochem 2006; 96: 766-776.

[27] Wang X, Chen JX, Liu YH, You C and Mao Q. Mutant TP53 enhances the resistance of glioblastoma cells to temozolomide by up-regulating O(6)-methylguanine DNA-methyltransferase. Neurol Sci 2013; 34: 1421-1428.

[28] Chen X, Tai L, Gao J, Qian J, Zhang M, Li B, Xie C, Lu L, Lu W and Lu W. A stapled peptide antagonist of MDM2 carried by polymeric micelles sensitizes glioblastoma to temozolomide treatment through p53 activation. J Control Release 2015; 218: 29-35.

[29] Kim SS, Rait A, Kim E, Pirollo KF, Nishida M, Farkas N, Dagata JA and Chang EH. A nanoparticle carrying the p53 gene targets tumors including cancer stem cells, sensitizes glioblastoma to chemotherapy and improves survival. ACS Nano 2014; 8: 5494-5514.

[30] Ostrom Q, Cohen ML, Ondracek A, Sloan A and Barnholtz-Sloan J. Gene markers in brain tumors: what the epileptologist should know. Epilepsia 2013; 54 Suppl 9: 25-29.

[31] Czapski B, Baluszek S, Herold-Mende C and Kaminska B. Clinical and immunological correlates of long term survival in glioblastoma. Contemp Oncol (Pozn) 2018; 22: 81-85.

[32] Braig M, Lee S, Loddenkemper C, Rudolph C, Peters AH, Schlegelberger B, Stein H, Dorken B, Jenuwein T and Schmitt CA. Oncogene-induced senescence as an initial barrier in lymphoma development. Nature 2005; 436: 660-665.

[33] Kuilman T, Michaloglou C, Mooi WJ and Peeper DS. The essence of senescence. Genes Dev 2010; 24: 2463-2479.

[34] Serrano M, Lin AW, McCurrach ME, Beach D and Lowe SW. Oncogenic ras provokes premature cell senescence associated with accumulation of p53 and p16INK4a. Cell 1997; 88: 593-602.

[35] Collin G, Huna A, Warnier M, Flaman JM and Bernard D. Transcriptional repression of DNA repair genes is a hallmark and a cause of cellular senescence. Cell Death Dis 2018; 9: 259.

[36] Eggert T, Wolter K, Ji J, Ma C, Yevsa T, Klotz S, Medina-Echeverz J, Longerich T, Forgues M, Reisinger F, Heikenwalder M, Wang XW, Zender L and Greten TF. Distinct functions of senescence-associated immune responses in liver tumor surveillance and tumor progression. Cancer Cell 2016; 30: 533-547.

[37] Meng D, Chen Y, Yun D, Zhao Y, Wang J, Xu T, Li X, Wang Y, Yuan L, Sun R, Song X, Huai C, Hu L, Yang S, Min T, Chen J, Chen H and Lu D. High expression of N-myc (and STAT) interactor predicts poor prognosis and promotes tumor growth in human glioblastoma. Oncotarget 2015; 6: 4901-4919.

Table S1. The relationship between the clinicopathologic characteristics and TRIM21 immunoreactivity in the Chinese TMA cohort

Characteristics	No. patient	TRIM21 expression		*P* value
		Low	High	
Gender				0.593
Male	178 (67.4%)	110 (61.8%)	68 (38.2%)	
Female	86 (32%)	50 (58.1%)	36 (41.9%)	
Age (year)				0.167
≥45	138 (52.3%)	78 (56.5%)	60 (43.5%)	
<45	126 (47.7%)	82 (65.1%)	44 (34.9%)	
Tumor origin				0.707
Primary	231 (87.5%)	141 (61%)	90 (39%)	
Secondary	33 (12.5%)	19 (57.6%)	14 (42.4%)	
Seizure				0.873
No	214 (81.1%)	129 (60.3%)	85 (39.7%)	
Yes	50 (18.9%)	31 (62%)	19 (38%)	
IICP				1.000
No	158 (59.8%)	96 (61%)	62 (39%)	
Yes	106 (40.2%)	64 (60.4%)	42 (39.6%)	
Cystic degeneration				0.051
No	204 (77.3%)	123 (60.3%)	81 (39.7%)	
Yes	50 (18.9%)	31 (62%)	19 (38%)	
Necrosis				0.441
No	232 (87.9%)	143 (61.6%)	89 (38.4%)	
Yes	32 (12.1%)	17 (53.1%)	15 (46.9%)	
MTD				0.450
<5	119 (45.1%)	69 (58%)	50 (42%)	
≥5	145 (54.9%)	91 (62.8%)	54 (37.2)	
Grade				**0.003**
LGG	103 (39%)	74 (71.8%)	29 (28.2%)	
HGG	161 (61%)	86 (53.4%)	75 (46.6%)	
Chemotherapy				0.508
No	91 (34.5%)	58 (63.7%)	33 (36.3%)	
Yes	173 (65.5%)	102 (59%)	71 (41%)	
Radiotherapy				0.347
No	86 (32.6%)	56 (65.1%)	30 (34.9%)	
Yes	178 (67.4%)	104 (58.4%)	74 (41.6%)	

Abbreviations: IICP, increased intracranial pressure; MTD, mean tumor diameter; LGG, low grade glioma; HGG, high grade glioma.

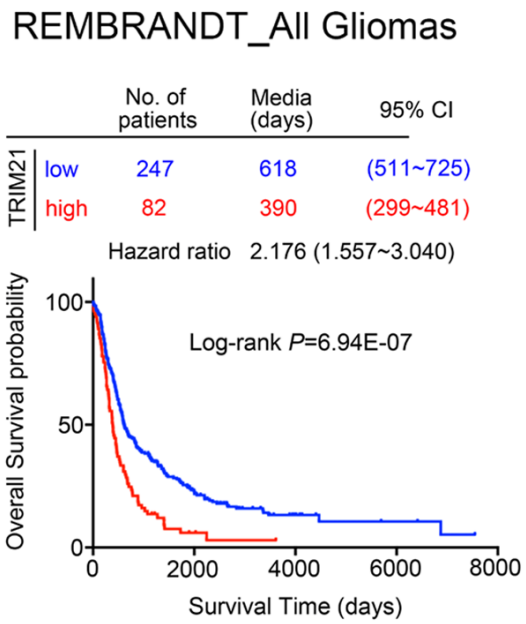

Figure S1. High expression of *TRIM21* predicts a poor clinical outcome in Rembrandt cohort. Kaplan-Meier survival curves were plotted according to different *TRIM21* gene expression for overall survival of all glioma patients in the Rembrandt cohort.

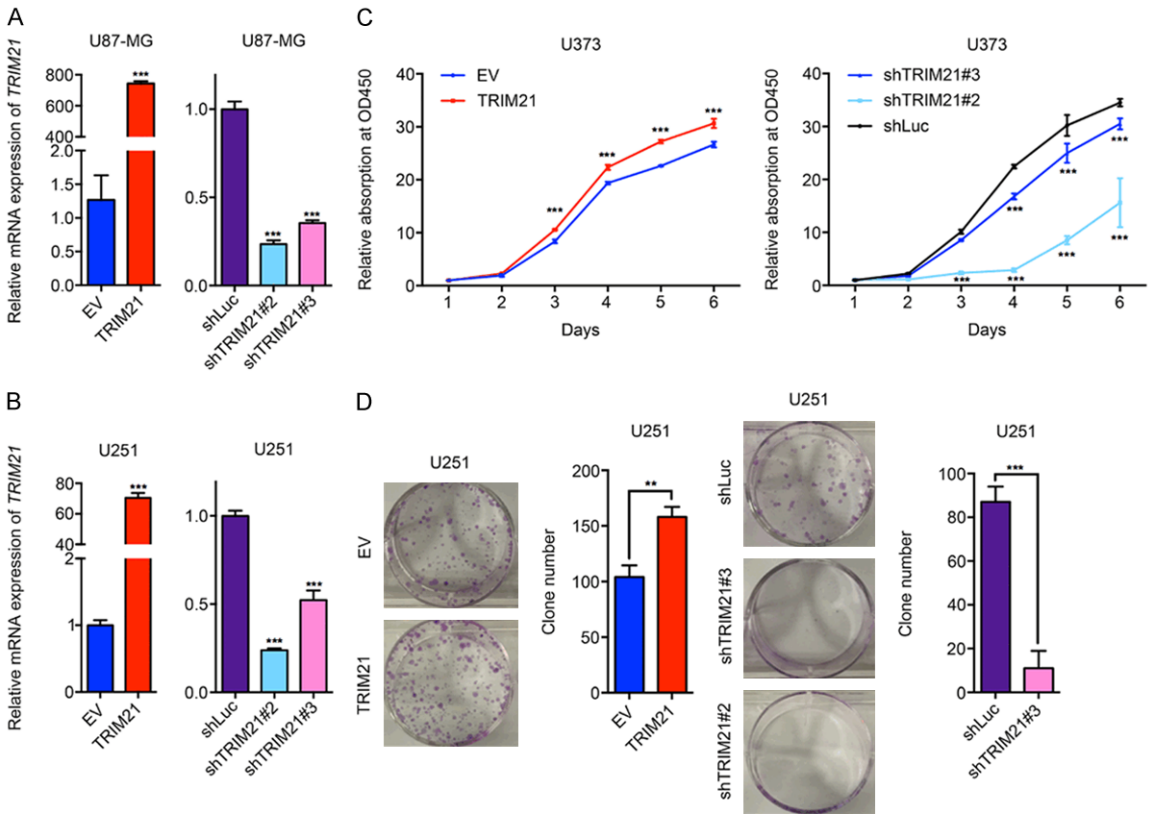

Figure S2. TRIM21 promotes glioma cell growth in vitro. (A, B) RT-qPCR assessments of *TRIM21* mRNA expression in U87-MG (A) or U251 (B) cells infected with lentivirus expressing indicated plasmids or shRNAs for 48 hr. Data are shown as means ± SD (n=3). ***, *P*<0.001. (C) CCK-8 cell proliferation analyses of U373 cells infected with lentivirus expressing indicated plasmids or shRNAs for 48 hr. Data are shown as means ± SD (n=3). ***, *P*<0.001. (D) Colony formation analyses of U251 cells infected with lentivirus expressing indicated plasmids or shRNAs for 48 hr. Data are shown as means ± SD (n=3). **, *P*<0.01; ***, *P*<0.001.

Table S2. The statistics summary of RNA-seq libraries

Library	Total reads	Reads length (bp)	Mapped reads	Mapping reads (%)
shLuc#1	17,457,159	300	15,808,446	90.56
shLuc#2	18,202,984	300	16,672,385	91.59
shLuc#3	20,961,171	300	19,226,848	91.73
shTRIM21#1	22,094,268	300	19,254,353	87.15
shTRIM21#2	20,833,814	300	17,871,792	85.78
shTRIM21#3	16,375,190	300	14,095,628	86.08

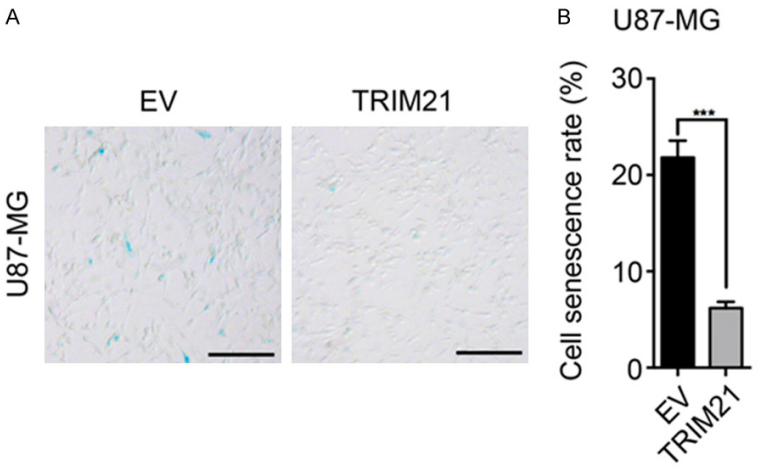

Figure S3. TRIM21 suppresses cell senescence in U87-MG cells. A. Representative images of SA-β-Gal staining of U87-MG cells infected with lentivirus expressing indicated plasmids for 48 hr. Scale bar, 50 μm. B. The quantitative analyses of SA-β-Gal staining assays. Data are shown as means ± SD (n=3). ***, $P<0.001$.